

AROUND THE EAST CHINA SEA FROM 2006 TO 2008

Dong-In Lee¹, Min Jang¹, Gil-Jong Seo¹, Dong-Soon Kim¹, Mi-Young Kang¹, Sang-Min Jang¹,
Min-Kyung Kim¹, Hiroshi Uyeda², Kazuhisa Tsuboki², Mariko Oue² and Cheol-Hwan You³

¹Department of Environmental Atmospheric Sciences, Pukyong National University, Busan, Korea

²Hydrospheric Atmospheric Research Center, Nagoya University, Nagoya, Japan

³Atmospheric Environmental Research Institute, Pukyong National University, Busan, Korea

1. INTRODUCTION

In summer season, the Korean peninsula, Japan, Taiwan and China are influenced several severe weather such as Changma/Baiu/Meiyu front, typhoon, strong low pressure, and local heavy precipitation. These are usually accompanied with heavy rainfall and strong wind which are one of the most significant factors in natural disasters. In addition, mesoscale convective systems during summer are well formed in a moist environment from the East China Sea and they are rapidly developed and produced heavy rainfall on each country.

To clarify the structure and formation process of these frontal precipitation systems, several experiments have been carried out in the East Asia. In Japan, observation studies of Doppler radars were carried out in Okinawa in 1987, Kyushu Island in 1988, and Kyushu Island and over the East China Sea between 1998 and 2002 (Ishihara et al., 1992; Ishihara et al., 1995; Takahashi et al., 1996; Yoshizaki et al., 2000). In China, the South China Sea Monsoon Experiment (SCSMEX) was carried out between 1996 and 2001 (Lau et al., 2000; Ding et al., 2004). The purpose of these experiments is to understand the mesoscale feature of frontal systems formed in the East Asia (Moteki et al., 2004). In Taiwan, TAMEX (Taiwan Area Mesoscale Experiments) was carried out around Taiwan in 1987 (Lin et al., 1991; Ray et al., 1991; Teng et al., 2000). In Korea, the KORMEX (Korean Mesoscale Experiment) was carried out in the middle of Korean peninsula in 1997 and 1998 (Oh et al., 1997) and the KEOP (Korean Enhanced Observing Program) was carried out in the southern part of Korean peninsula from 2001 to present (Choi and Nam, 2006).

Especially in Korean peninsula, these observational studies are very important because more than half of

annual precipitation over the Korean peninsula is occurred during the summer and the Changma front accompanies with a belt-like peak rainfall zone which developed from the convergence zone between the tropical maritime air mass from the south and both continental and maritime polar one from the north (Oh et al., 1997). Some heavy rainfall in Korea is developed from mesoscale disturbances which originated in China and then propagated eastward along the frontal system. There have been also many studies on the synoptic conditions of this heavy rainfall (Kim et al., 1983; Lee et al., 1998). Lee et al. (1998) analyzed 10 heavy rainfall cases from June to July during 1980-1990. They found that the upper-level and the low-level jets, lower level vorticity, high equivalent potential temperature and moisture field can produce heavy rainfall. However other additional factors are important parameters to clarify the heavy rainfall development mechanism in Changma season. Many previous studies have been conducted to analyze the mechanism of heavy rainfall in Changma season. In Korea, the observation studies using radar data, focused on the Changma front for the analysis of its background field and additional factors such as the microphysical features and kinematic characteristics of wind fields at lower latitude of the Korean peninsula had been rarely conducted.

Therefore, from June, 2006 to now around the East China Sea, we have performed several intensive observations for the purpose of the prevention from disaster caused by severe weather and the understanding of those mechanisms. In this study, our activities on the field observation will be introduced and one of results will be explained.

2. EXPERIMENTAL DESIGN AND METHOD

The first experiment was carried out in Jeju Island and Marado of Korea in summer, 2006. The second field experiment was conducted in Okinawa, Japan with Nagoya University in June, 2007. The third and fourth intensive experiments were performed in Jeju and Chujado of Korea in June and July, 2007, respectively. In 2008, we participated in the intensive observation related with SoWMEX/TiMREX

* Corresponding author address: Dong-In Lee, Dept. of Env. Atmos. Sci., Pukyong National University, Nam-gu, Busan, 608-737, Korea
E-mail: leedi@pknu.ac.kr

(Southwest Monsoon Experiment/Terrain-influenced Monsoon Rainfall Experiment) in Taiwan for understanding East Asian monsoon system and carried out the field experiment in leodo of Korea. These observation stations are good observation bases, since they have a moisture environmental condition and geographical location belonged trace of typhoon (Fig. 1).

During the observation periods, we installed several instruments such as POSS (Precipitation Occurrence Sensor System), AWS (Automatic Weather Systems), rain gages, radiosonde, filter paper for DSD, LPC (Laser Particle Counter) and so on.

Dual Doppler radar analysis was used to know the kinematic characteristics of precipitation system, and synoptic analysis was accomplished by NCEP/NCAR reanalysis data. In order to understand the strength of temperature gradient and warm or cold advection the total vertical wind shear (here after, TVWS) and directional vertical wind shear(here after, DVWS) were calculated by radiosonde data, respectively (Neiman, 2003). The temperature gradient and the advection are approximated from geostrophic thermal wind equation (Holton, 1979) on the isobaric layer. If the geostrophic VWS is assumed to be the observed VWS, the temperature gradient and the advection can be calculated from the equation (1) and (2). It means that the TVWS is proportional to the strength of the temperature gradient and the positive (negative) DVWS is related to the warm (cold) advection.

$$\left| \frac{dV}{dz} \right| \equiv \sqrt{\left(\frac{du}{dz} \right)^2 + \left(\frac{dv}{dz} \right)^2} \quad (1),$$

$$\frac{dD}{dz} \equiv -\left(u \frac{dv}{dz} - v \frac{du}{dz} \right) \quad (2)$$

where, $V = u\hat{i} + v\hat{j}$, $\bar{u} = (u(k+1) + u(k-1))/2$, $\bar{v} = (v(k+1) + v(k-1))/2$, k is the vertical layer and dz is 500 m in this study.

To know the drop size distributions of rainfall accompanied with Changma front, gamma distribution fit using 3rd, 4th, 6th moments was used (Ulbrich, 1983; Kozu and Nakamura, 1991). To better express the drop size distributions, many researchers used the general gamma distribution as follows;

$$N(D) = N_0 D^m \exp(-\Lambda D) \quad (3)$$

where, N_0 , D , m , and Λ are represent intercept, diameter of rain drop, shape, and slope, respectively. The DSDs were obtained from POSS which has 34 channels from 0.34 mm to 5.34 mm.

3. RESULTS

Especially during intensive observation period in 2007, rainfall system on 5th and 6th July was selected because of its heavy rainfall amount. The precipitation

system had 20 hour duration totally and recorded rainfall amount over 138.4 mm (in Fig. 2). It was caused by Changma front accompanied with strong low pressure as shown in Fig. 3. The rainfall occurred at this time had different direction of movement before and after passing through Chujado and short break at certain time period. And the vertical profile of temporal reflectivity at Chujado area was calculated from Gosan S-band weather radar (Fig. 4). Three different rainfall systems were categorized using animated Gosan radar data as follows (not shown here); in case 1, rainfall system moved from north-west and went into the south-east after passing through Chujado. After very short break, rainfall system in case 2 became weaker and moved to almost east. After short break again, it was originated in the west or north-west of Chujado and moved to the east or north-east.

The surface weather map shows that southerly wind was flowed into Chujado area due to the low pressure located at the western part of Jeju Island (Fig. 5(a)). Low pressure with southerly wind and high pressure with north-northwesterly wind located at the East Sea or Japan Sea which was converged at the central part of the Korean peninsula. In the 850 hPa layer on Fig. 6(b), a strong wind higher than 15 ms^{-1} was dominated over the whole southern part of Korea. The gradient of equivalent potential temperature around 12 K was large at the south-western part of Jeju Island. Vertical strong wind shear would be occurred since horizontal wind was westerly at 500 and 300hPa and south-westerly at surface level.

Figure 6 shows the TVWS and DVWS obtained from radio sondes at 2100 KST on 5 July, 0300 KST, and 0900 KST on 6 July. At 2100 KST on 5 July, the TVWS was 10.7 m/s/km around 1 km and became weaker with the increase of altitude. The DVWSs were -3.3 degrees/km, 68.2 degrees/km, -40.1 degrees/km, and 41.2 degrees/km at 1km, 2 km, 3km, and 4 km, respectively. It means that the cold (warm) advection appeared at 1 km and 3 km (2 km and higher than 4 km). At 0300 KST on 6 July, 19.3 and 13.9 m/s/km of TVWS located at the height of 1 km and 3 km, respectively. The DVWS was 20.9 degrees/km at 1 km, -11.2 degrees/km at 2 km, and 186.9 degrees/km at 3 km. It means that the warm (cold) advection dominated at the height of 1 km, 3km, 4 km and 5 km (2 km and 6 km). At 0900 KST on 6 July, the TVWS was 20.7 m/s/km around surface and decreased with increase of height. The DVWS was 108.2 degrees/km at the height of 1 km and the positive DVWS dominated in the whole layer, which means the warm advection was significant at all layers.

Wind fields obtained from dual Doppler analysis are represented from Figure 8 to 10. At 2300 KST, horizontal convergence between south-westerly and westerly occurred at the western part of Chujado. The rainfall system moves into north-eastern part (Fig. 7(a)). In the range of 10 to 30 km on the vertical cross section of A-A' line in Figure 8(a), strong updraft and downdraft more than 10 ms^{-1} are repeated (Fig. 7(b)). The echo top of 30 dBZ is nearly 6 km in height and strong south-westerly winds about 30 ms^{-1} is identified around 20 km in distance (Fig. 7(c)). The convergence are from -10 to $-30 \times 10^{-4} \text{ s}^{-1}$ and horizontal vorticity is $-20 \times 10^{-4} \text{ s}^{-1}$ within 20 km from "A" point (Fig. 7(d)). The updraft, convergence, and horizontal vorticity near Chujado were around 5 m s^{-1} , $-10 \times 10^{-4} \text{ s}^{-1}$, and -5 to $15 \times 10^{-4} \text{ s}^{-1}$, respectively.

In case 2, the precipitation system with relatively weaker intensity and wind speed than at case 1 moved into the east (Fig. 8(a)). The downdraft less than 4 ms^{-1} was dominated within 20 km from A as shown in Fig. 8(b). The echo top of 30 dBZ was located around 4 km and the wind direction with height was almost constant (Fig. 8(c)). The convergence around was not significant and horizontal vorticity was $-15 \times 10^{-4} \text{ s}^{-1}$ within the range of 20 km from "A" (Fig. 8(d)). The updraft and horizontal vorticity near Chujado were around 3 ms^{-1} and -10 to $15 \times 10^{-4} \text{ s}^{-1}$, respectively.

In case 3, rainfall system moves to the east or north-eastward and strong wind speed flowed more than 15 ms^{-1} (Fig. 9(a)). The downdraft and updraft with 4 to 6 ms^{-1} was occurred within 20 km and 30 dBZ echo top was existed around 6 km in height (Fig. 9(b)). In Fig. 9(c), south-westerly winds flowed at the surface and higher north-westerly winds than 15 ms^{-1} flowed at the range of 40 km from "A". The divergence with $-10 \times 10^{-4} \text{ s}^{-1}$ was occurred till the 3 km in height in range from "A" (Fig. 9(d)). The updraft, convergence, and horizontal vorticity near Chujado were around 3 m s^{-1} , $-10 \times 10^{-4} \text{ s}^{-1}$, and -10 to $5 \times 10^{-4} \text{ s}^{-1}$, respectively.

Figure 10 shows that the time series of rainrate and number concentration with size. The maximum rainrates for one minute of each case were 113.6, 18.1 and 224.3 mmh^{-1} , respectively. The drop numbers of rain drop less than or equal to 2 mm and larger than 2 mm were very different with cases. Fig. 11 shows that the averaged DSDs obtained from a POSS disdrometer and gamma model, respectively. The mean rainrate of each case was 6.14, 2.92, and 9.44 mm/h. In all cases, the shape of DSDs had the exponential fitting except for smaller drop sizes.

However, there is a significant difference of number concentrations at before and after 2 mm drop in diameter between case 1 and case 3. The drops smaller than 2 mm in diameter were contributed to case 3 and larger ones than 2 mm were contributed to

the case 1. This tendency was also shown in Fig. 11(b). It is considered in simple sense that rain drops in case 1 would be affected by coalescence which decreases the numbers of small size drops and increases those of the larger drops. The DSDs in case 3 would be affected by collisional break-up which increases the numbers of small size drops and decreases the numbers of big size drops.

4. SUMMARY

To understand and clarify the structure and development processes of precipitation system on the Changma frontal region, intensive observation experiments were carried out. The three rainfall cases within one precipitation system were selected (from 5 to 6 July in 2007) and analyzed by using rain gauge data, radio sonde data, POSS, weather radar and NCEP/NCAR reanalysis data.

The deep warm advection was proved to make rainfall system maintained for longer time and stronger rainrate but smaller size diameter of raindrop was contributed as shown in case 3. The unstable instability, which means the cold advection at the surface and the warm advection at higher layer, would make larger size diameter of raindrop contributed to the rainfall system as occurred in case 1. The characteristics of meso scale precipitation system might be further valid by analyzing the system for shorter time and focusing on the precipitation appearance like band shape type with its orientation as it is propagating.

In the future, we will focus on the observation and data collection continuously to obtain more valuable data and investigate the mechanism of severe weather phenomena such as heavy rainfall, gust fronts and typhoon.

5. ACKNOWLEDGMENTS

This work was supported by the Korea Foundation for International Cooperation of Science & Technology (KICOS) through a grant provided by the Korean Ministry of Education, Science & Technology (MEST) in 2008 (No. K2 0607010001-08A050100110). This work was partly supported by the second stage of Brain Korea 21 Project.

6. REFERENCES

- Choi, Y.J. and J.C., Nam, 2006: Introduction of phase I KEOP., Proceedings of the spring meeting of KMS, 384-385(In Korean).
- Ding, Y.H., C.Y. Li and Y.J. Liu, 2004: Overview of the South China Sea monsoon experiment. Adv.

Atmos. Sci., 21, 343-360.

Holton, J. R., 1979: An introduction to dynamic meteorology. Academic Press, 391 pp.

Ishihara, M., A. Tabata, K. Akaeda, T. Yokoyama and H. Sakakibara, 1992: The structure of a subtropical squall line observed with a Doppler radar, *Tenki*, 39, 727-743 (in Japanese)

Ishihara, M., Y. Fujiyoshi, A. Tabata, H. Sakakibara, K. Akaeda and H. Okamura, 1995: Dual Doppler radar analysis of an intense mesoscale rainband generated along the Baiu front in 1988: Its kinematical structure and maintenance process. *J. Meteor. Soc. Japan*, 73, 139-163.

Kim, S.S., C.H. Chung, S.U. Park, and B.S. Lee, 1983: The characteristic structural differences of the rainy front (Changma front) between the wet and dry seasons. *J. Korean Meteor. Soc.*, 19, 12-32 (in Korean).

Kozu, T. and K. Nakamura, 1991: Rainfall parameter estimation from dual-radar measurements combining reflectivity profile and path-integrated attenuation. *J. Atmos. Oceanic Technol.*, 8, 259-271.

Lau, K.M., Y.H. Ding, J.T. Wang, R. Johnson, R. Cifelli, J. Gerlach, O. Thjiely, T. Rikebbach, S.C. Tsay and P.H. Lin, 2000: A report of the field operation and early results of the South China Sea monsoon experiment (SCSMEX). *Bull. Amer. Meteor. Soc.*, 81, 1261-1270.

Lee, D.K., H.R. Kim, and S.Y. Hong, 1998: Heavy rainfall over Korea during 1980-1990. *Kor. J. of Atmos. Sci.*, 1, 32-50.

Lin, Y.-J., R.W. Pasken and H.-W. Chang, 1991: The structure of a subtropical prefrontal convective rainband. Part I: Mesoscale kinematic structure determined from dual Doppler measurements. *Mon. Wea. Rev.*, 120, 1816-1836.

Moteki, Q., H. Uyeda, T. Maesaks, T. Shinoda, M. Yoshizaki, and T. Kato, 2004: Structure and development of two merged rainbands observed over the East China Sea during X-BAIU-99 PART I: Meso- β -scale structure and development processes. *J. Meteor. Soc. Japan*, 82, 19-24.

Nieman, P. J., 2003: Private communication.

Oh, J.H., W.T. Kwon, and S.B. Ryoo, 1997: Review of the researches on Changma and future observational study (KORMEX). *Adv. Atmos. Sci.*, 14, 207-222.

Ray, P.S., A. Robinson and Y. Lin, 1991: Radar analysis of a TAMEX frontal system. *Mon. Wea.*

Rev., 119, 2519-2539.

Takahashi, N., H. Uyeda, K. Kikuchi and K. Iwanami, 1996: Mesoscale and convective scale features of heavy rainfall events in lat period of the Baiu season in July 1988, Nagasaki Prefecture. *J. Meteor. Soc. Japan*, 74, 539-561.

Teng, J.-H., C.-S. Chen, T.-C.C. Wang and Y.-L. Chen, 2000: Orographic effects on a squall line system over Taiwan. *Mon. Wea. Rev.*, 128, 1123-1138.

Ulbrich, C. W., 1983: Natural variations in the analytical form of the raindrop size distribution. *J. Climate Appl. Meteor.*, 22, 1764-1775.

Yoshizaki, M., T. Kato, Y. Tanaka, H. Takayama, Y. Shoji, H. Seko, K. Arai, K. Manabe and Members of X-BAIU-98 Observation, 2000: Analytical and numerical study of the 26 June 1998 orographic rainband observed in Western Kyushu, Japan. *J. Meteor. Soc. Japan*, 78, 835-856.

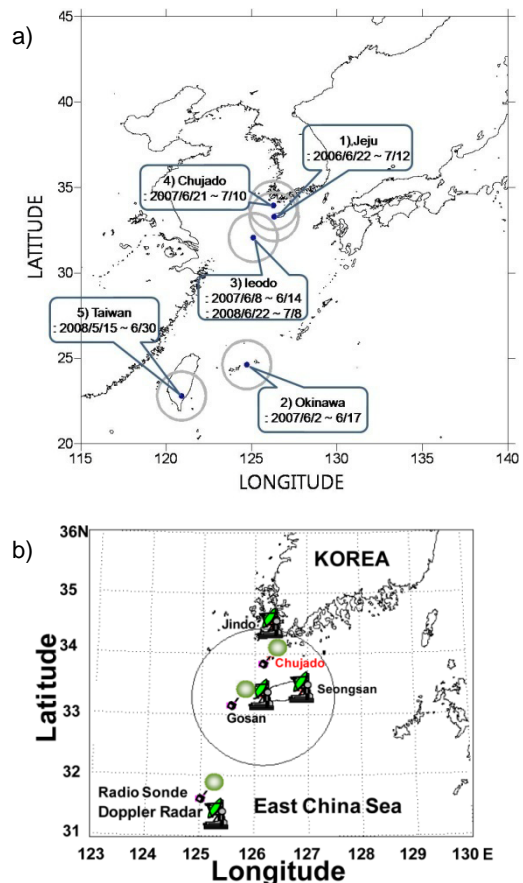


Fig. 1. a) The location of field experiments from 2006 to 2008, b) Doppler weather radar and radiosonde launched in 2007.

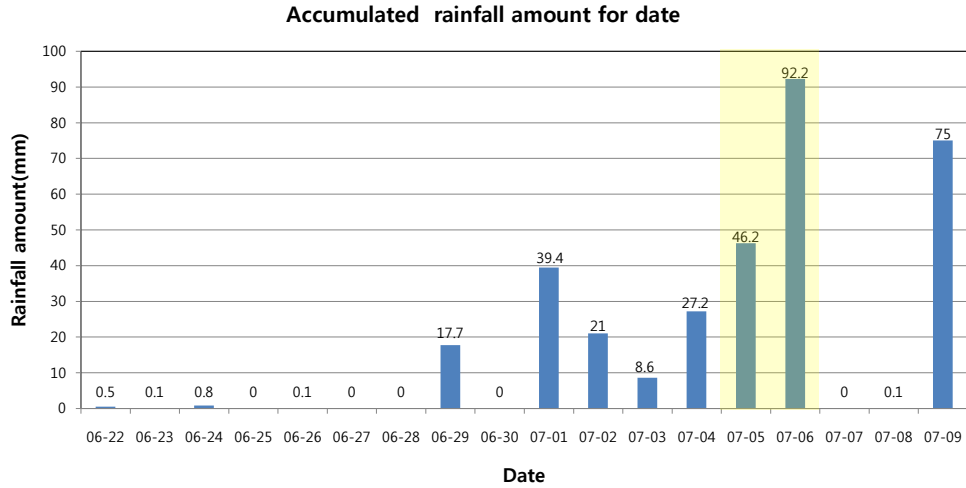


Fig. 2. Rainfall amount of Chujado during intensive observation period in 2007.

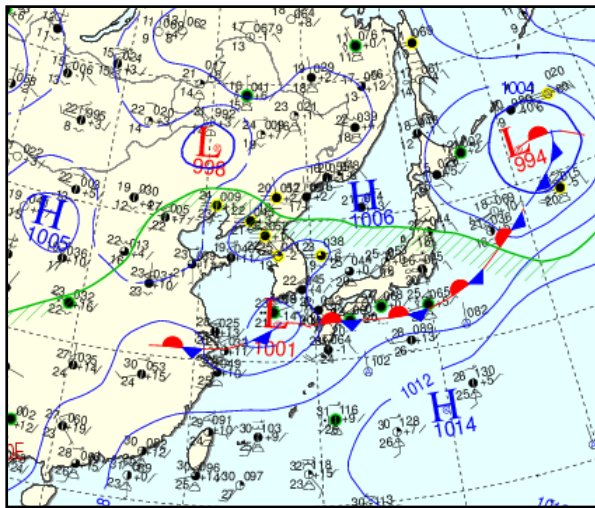


Fig. 3. The surface weather chart on 0900 KST, 6th July in 2007.

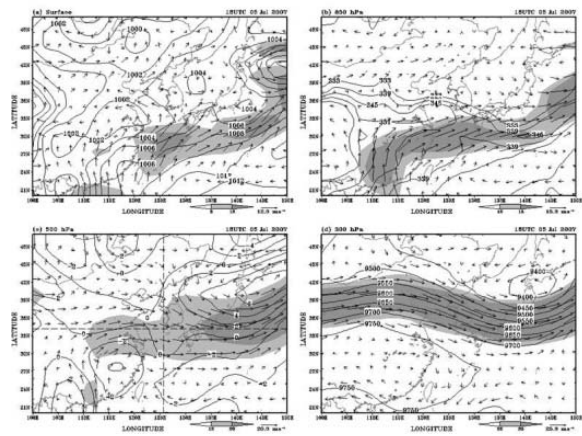


Fig. 5. (a) Pressure and wind vector at surface, (b) equivalent potential temperature and wind vector at 850hPa, (c) relative vorticity and wind vector at 500hPa, (d) geopotential height and wind vector at 300hPa 0300 KST on 6th July in 2007.

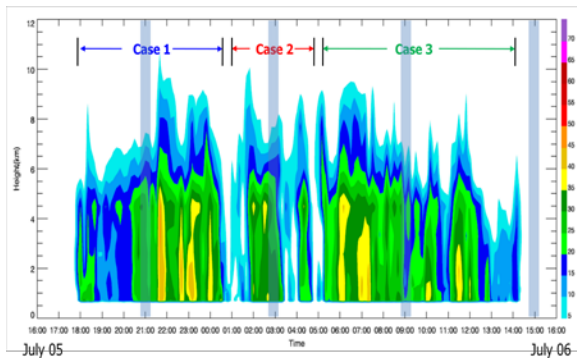


Fig. 4. The vertical profile of temporal reflectivity with time at Chujado from Gosan weather radar. Blue shaded boxes show the time launched radio sondes.

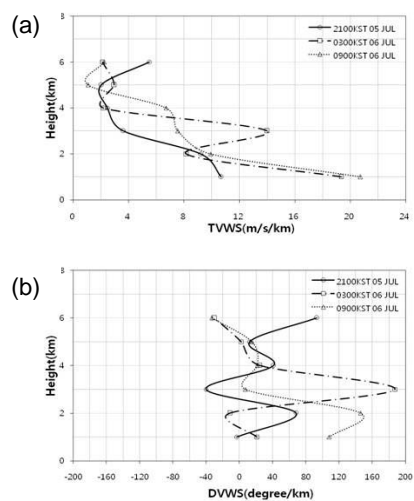


Fig. 6. The total vertical wind shear (TVWS, (a)) and directional vertical wind shear (DVWS, (b)) obtained from radio sondes.

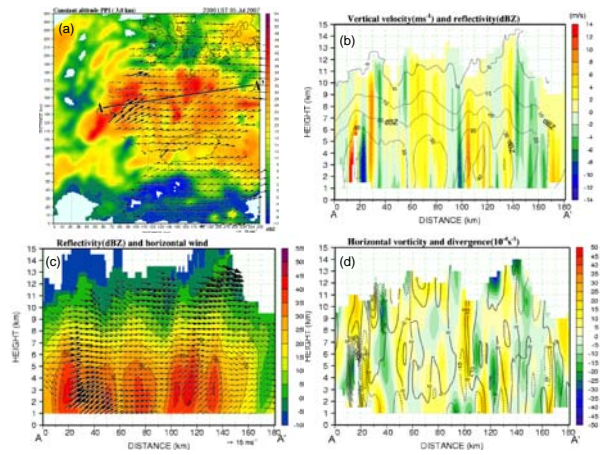


Fig. 7. (a) The reflectivity and horizontal wind field at the 3 km CAPPI at 2300 KST 5 July in 2007. Vertical cross sections along A-A' in (a) vertical velocity and reflectivity (b), horizontal wind and reflectivity (c), and horizontal vorticity and divergence (d).

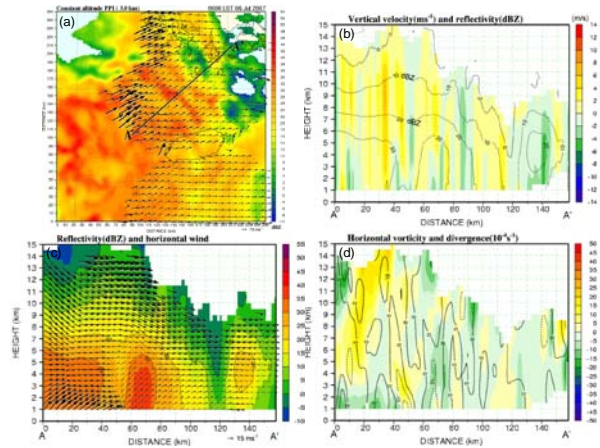


Fig. 8. The same as Fig. 7 but for 0300 KST 6 July.

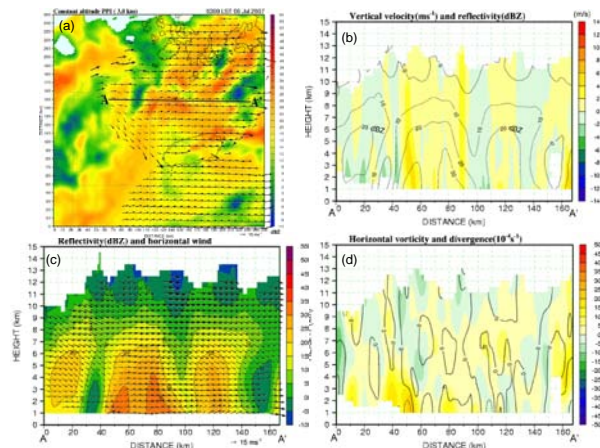


Fig. 9. The Same as Fig. 7 but for 0600 KST 6 July.

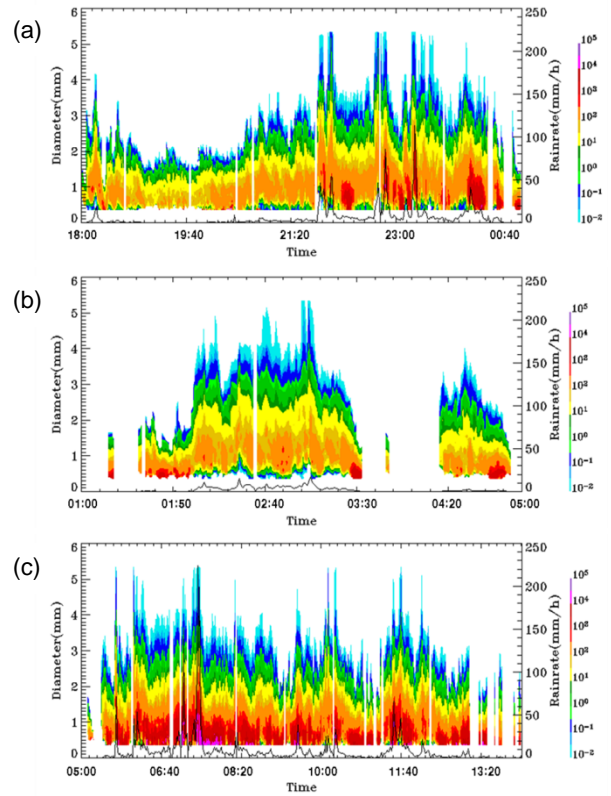


Fig. 10. The time series of rain drop size (left axis) and rainrate (right axis) derived from POSS (a) case 1, (b) case 2, and (c) case 3.

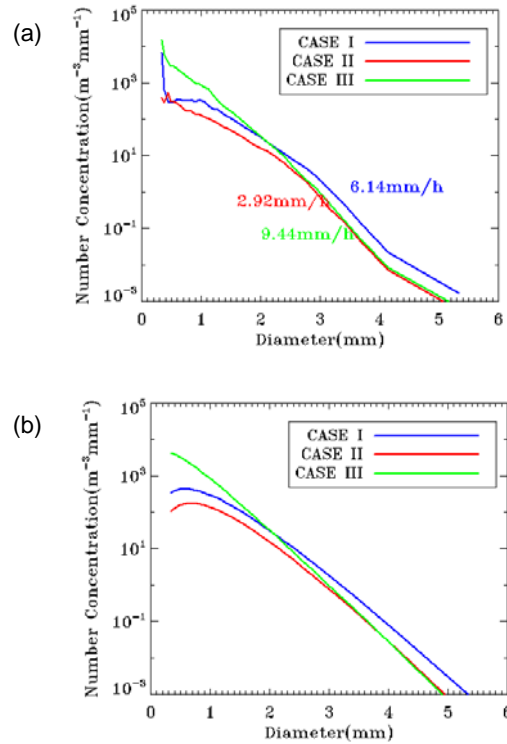


Fig. 11. Averaged DSD from (a) POSS disdrometer and (b) gamma distribution.